Available online at www.sciencedirect.com
ScienceDirect
Trans. Nonferrous Met. Soc. China 25(2015) 3012−3022
Transactions of Nonferrous Metals Society of China
www.tnmsc.cn

Amorphous SiO_2 interlayers for deposition of adherent diamond films onto WC−Co inserts

Yu-xiao CUI, Tian-qi ZHAO, Fang-hong SUN, Bin SHEN

State Key Laboratory of Mechanical System and Vibration, School of Mechanical Engineering, Shanghai Jiao Tong University, Shanghai 200240, China

Received 15 October 2014; accepted 20 June 2015

Abstract: Amorphous SiO_2 (a-SiO_2) films were synthesized on WC−Co substrates with H_2 and tetraethoxysilane (TEOS) via pyrolysis of molecular precursor. X-ray diffraction (XRD) pattern shows that silicon−cobalt compounds form at the interface between a-SiO_2 films and WC−Co substrates. Moreover, it is observed by transmission electron microscope (TEM) that the a-SiO_2 films are composed of hollow mirco-spheroid a-SiO_2 particles. Subsequently，the a-SiO_2 films are used as intermediate films and chemical vapor deposition (CVD) diamond films are deposited on them. Indentation tests were performed to evaluate the adhesion of bi-layer (a-SiO_2 + diamond) films on cemented carbide substrates. And the cutting performance of bi-layer (a-SiO_2 + diamond) coated inserts was evaluated by machining the glass fiber reinforced plastic (GFRP). The results show that a-SiO_2 interlayers can greatly improve the adhesive strength of diamond films on cemented carbide inserts; furthermore, thickness of the a-SiO_2 interlayers plays a significant role in their effectiveness on adhesion enhancement of diamond films.
Key words: hot filament chemical vapor deposition (HFCVD); diamond film; WC−Co substrate; interlayer; adhesion

1 Introduction

Owing to the unique characteristics of chemical vapor deposition (CVD) diamond films, such as low thermal expansion coefficient, low friction, good thermal conductivity, excellent wear resistance and high hardness, WC−Co cemented carbide cutting tools coated with diamond films have shown great potentialities in machining metal−compound materials, non-ferrous metals and alloys, carbon fiber reinforced plastics (CFRP), printed circuit boards (PCBs) and hard brittle non-metals (for instance, ceramics and graphite) [1]. However, the adhesion between diamond films and WC−Co substrates, which is of great importance to the lifetime of diamond coated tools, needs to be further improved. The binder phase is detrimental to diamond nucleation and growth due to the catalytic graphitization behavior of metallic cobalt during CVD process, which causes severe interfacial graphitization [2]. Besides, the mismatch of thermal expansion coefficient can result in rather high residual stress at the interface of film−substrate system. This is another reason for the adhesion failure of diamond film [3].

Many types of pre-treatments have been performed to decrease the influence of binder phase Co and enhance the adhesive strength of diamond films on cemented carbide substrates in the published literatures [4−6]. Among them chemical etching of binder phase is one of the most popular pre-treatments used in industry [7]. However, sometimes the removal of binder phase can cause a porous, brittle and Co-depleted carbide layer on the substrate surface, which will lead to the deterioration of interfacial adhesion of film−substrate system. Moreover, during CVD diamond deposition, the metallic Co can diffuse from the bulk to WC−Co substrate surface continuously, which will cause the growth of graphite phases [3].

Another widely used method is to fabricate a barrier layer, which can prevent the catalytic effect of Co and meanwhile relieve the mismatch of thermal expansion. For the past decades, various interlayers, ranging from DLC [8], metals [9], ceramics [10] to their multilayer films [11], have been studied and reported. According to these researches, considerable success has been made in obtaining adhesion improvement of diamond coatings on cemented carbide tools by employing interlayers. And several authors give subsequent machining data of the

Foundation item: Project (20130073110036) supported by the Research Fund for the Doctoral Program of Higher Education of China
Corresponding author: Fang-hong SUN; Tel: +86-21-34206557; Fax: +86-21-62932610; E-mail: sunfanghong@sjtu.edu.cn
DOI: 10.1016/S1003-6326(15)63928-0

interlayered diamond films, thus confirming that certain interlayers have a quite positive effect on tool life [9,12].

Amorphous ceramic is in good grace from wide aspects, considering yield strength, break strength, abrasive resistance, corrosion resistance and thermal characteristic [13], which makes it a very promising interlayer material. However, up to now there are only a few data concerning the application of amorphous ceramic interlayers on the fabrication of CVD diamond films. ENDLER et al [8] synthesized a-SiC, a-Si_3N_4 and a-SiC_xN_y interlayers by CVD and performed diamond deposition on those amorphous interlayers. For industrial application, however, the influence of amorphous interlayers on the cutting performance of diamond films remains an issue. Further study on the amorphous interlayers is needed.

It has been proved that polycrystalline diamond films can be deposited on SiO_2 [14]. In this work, on the basis of two-step chemical pre-treatment, a-SiO_2 interlayers with various growth durations were prepared by thermal decomposition of TEOS using a self-made CVD apparatus. Subsequently, the diamond films were deposited on as-fabricated a-SiO_2 interlayers in a home-made HFCVD apparatus. Then, cutting tests against glass fiber reinforced plastics (GFRP) were performed to investigate the influence of a-SiO_2 interlayers on the cutting performance of CVD diamond coated inserts. Our findings were compared with the result from the diamond coated insert without interlayer. The research results show that the a-SiO_2 interlayers can improve the interfacial adhesion of diamond film−substrate system, and the effectiveness of a-SiO_2 interlayers is dramatically affected by their growth duration.

2 Experimental

The WC−6%Co cemented carbide inserts were used as substrate in this study. The average WC grain size was 1.5 μm. First, they were ultrasonically cleaned in acetone to remove the surface impurities. And then they were submitted to a two-step pretreatment to remove the surface binder phase and roughen the substrate surface as well. The inserts were dipped in the Murakami's regent (10 g $K_3[Fe(CN)]_6$ + 10 g KOH + 100 mL H_2O) in ultrasonic vessel for 15 min [7]; then, the surface binder phases were washed away in the acid (30 mL H_2SO_4 + 70 mL H_2O_2) for 1 min. In order to reduce the catalytic effect of residual binder phase and improve the interfacial adhesion of film−substrate system, the chemical etched WC−Co substrates were ultrasonically cleaned in acetone and subsequently coated with a-SiO_2 intermediate films by pyrolysis of TEOS. The a-SiO_2 deposition was performed by a self-made thermal decomposition reactor, with TEOS and hydrogen as reactant gas. The deposition parameters of a-SiO_2 interlayers are listed in Table 1. After the deposition of a-SiO_2 interlayers, WC−Co substrates were then diamond coated using a home-made HFCVD reactor, with six tantalum filaments as hot filaments. The tantalum filaments were carburized prior to CVD process. The reactant gases were H_2 and acetone. The deposition parameters of diamond film are listed in Table 2. For the sake of comparison, diamond film was also synthesized on chemical etched WC−Co insert without interlayer, which was abraded with 5 μm diamond powder suspension and ultrasonically cleaned in acetone before CVD process.

The different deposition processes on cemented carbide inserts are shown in Table 3.

Field emission gun scanning electron microscopy (FEG-SEM) was used to investigate the morphologies of a-SiO_2 films and CVD diamond films. Energy dispersive X-ray spectroscopy (EDX) measurements were used to give an elemental analysis of the a-SiO_2 interlayer coated substrates and conventional chemical etched substrates. X-ray diffraction (XRD) was adopted to detect the formation of a-SiO_2. In addition, the interlayer material was investigated by transmission electron microscopy (TEM) to further study the microstructure of a-SiO_2 interlayer. The interlayer material was mixed with alcohol, and it was ground into sub-microscale regimes in a mortar and pestle. Subsequently, the turbid liquid with ground interlayer material was placed in a

Table 1 Deposition parameters of a-SiO_2 interlayer

Pressure/ Pa	Gas flow/ ($mL \cdot s^{-1}$)	V(TEOS)/V(H_2)/%	Filament−substrate distance/mm	Filament temperature/°C	Substrate temperature/°C
1599.864	100	0.5	15	2200	700

Table 2 Deposition parameters of diamond film

Deposition	Pressure/ Pa	Gas flow/ ($mL \cdot s^{-1}$)	V(Acetone)/V(H_2)/%	Filament−substrate distance/mm	Filament temperature/°C	Substrate temperature/°C	Negative bias current/A
Nucleation	1999.83	300	1	10	2200	800	4
Growth	3999.66	300	1	10	2200	800	4

Table 3 Different deposition processes for WC−Co cemented carbide substrates

Specimen No.	a-SiO_2 interlayer growth duration/min	Diamond deposition	
		Nucleation time/h	Growth time/h
A	–	–	–
B	20	−	−
C	40	−	−
D	60	−	−
E	−	0.5	3.5
F	20	0.5	3.5
G	40	0.5	3.5
H	60	0.5	3.5

ultrasonic vessel for 15 min to be well mixed. After that 50 μL of the turbid liquid was dropped onto carbon film, which was mounted on copper grid as support. The carbon film with turbid liquid was dried under a lamp for 30 min. Then, the carbon film was placed in the vacuum cavity and the microstructure of ground interlayer material was detected by TEM. Micro-Raman scattering was adopted to investigate the composition of CVD diamond films and evaluate their residual stresses, which was excited by 632.8 nm He−Ne laser light. The adhesion evaluation of as-fabricated diamond films on cemented carbide inserts was performed on a Rockwell hardness tester with constant load of 100 kg. The indentation on each specimen was investigated by SEM.

Cutting tests were performed to check the influence of a-SiO_2 interlayers on the cutting behavior of as-fabricated bi-layer coated inserts. The work piece was a solid rod of glass fiber reinforced plastics (GFRP), whose details were given in Ref. [15]. During machining tests the cutting velocity was set at 280 m/min, with depth of cut kept at 0.05 mm and feed rate of 0.1 mm/r. After each cutting pass, the insert flank wear was examined by measuring the scars that appear on the cutting edge by optical microscope [15,16]. Also, the ultimate flank wear of tested inserts was characterized by SEM.

3 Results

3.1 Characterization of a-SiO_2 intermediate films

Figure 1 shows the SEM images of surface topography of a-SiO_2 films with different deposition time on two-step pre-treated WC−Co cemented carbide inserts. As can be seen in Fig. 1(a), after chemical etching, the surface binder phase of cemented carbide insert is remarkably etched and washed away. Moreover, the surface is obviously roughened after the two-step etching. The morphology presents a rugged surface, which is covered with WC grains. This illustrates the typical morphology of cemented carbide after two-step chemical etching. According to Fig. 1(b), mud-like a-SiO_2 is deposited on WC−Co substrate. The substrate surface is partly covered by the amorphous material, whose original morphology can be clearly recognized. As the growth time of interlayer reaches 40 min, the sharp edges and corners of WC grains are wrapped by the a-SiO_2 material. This leads to the surface morphology of the specimen close in texture with

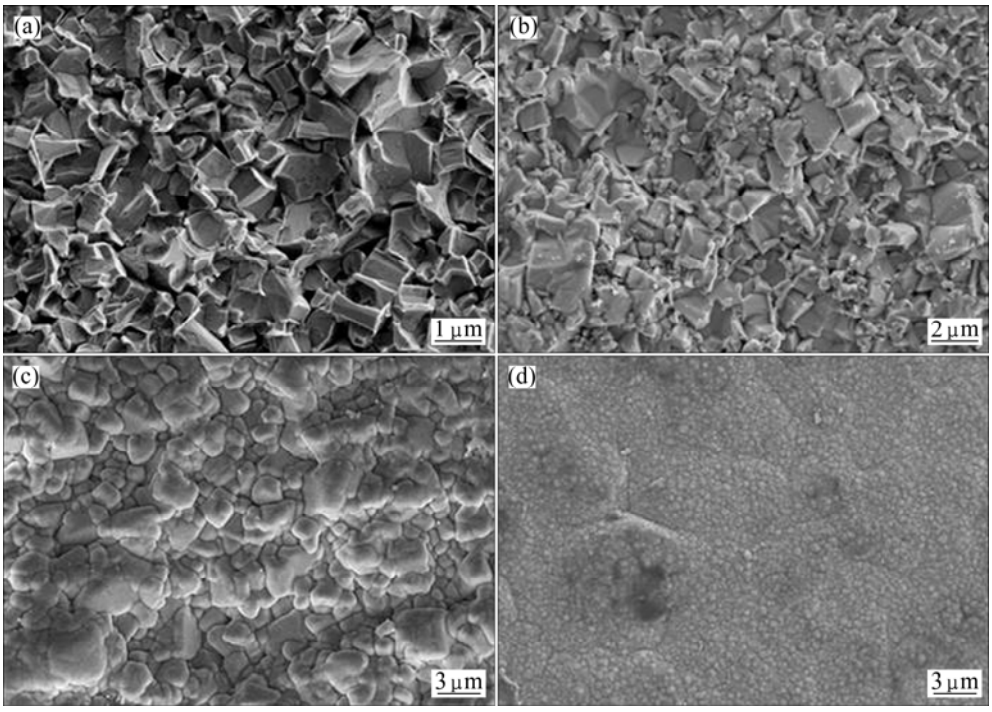

Fig. 1 SEM images of surface topography: (a) Specimen A; (b) Specimen B; (c) Specimen C; (d) Specimen D

ball-like appearance (Fig. 1(c)). Nevertheless, when the growth time of interlayer reaches 60 min, the original rugged WC−Co substrate surface can no longer be recognized. The chocolate-like image of the electron micrographs appears to be amorphous nature of the film, which indicates a homogeneous microstructure in the a-SiO_2 film (Fig. 1(d)).

Figure 2 shows the element compositions of two-step pre-treated substrates with or without a-SiO_2 films detected by EDX microanalyses. In Fig. 2(a), the intense peak of W shows the main ingredient of WC−Co substrate, and the weak Co peak reveals the incomplete removal of binder phase from the specimen by the chemical etching used in this study. Besides, the high temperature of CVD process can give rise to a strong Co migration from the bulk toward the substrate surface as well [17]. These drawbacks will lead to the formation of graphite carbon at the interface between diamond films and cemented carbide substrates and reduce the adhesion of diamond films on cemented carbide inserts. According to Figs. 2(b)−(d), the Co is strongly reduced in the surface zone. Co remains in the WC−Co substrates and does not diffuse into the interlayers. Therefore, metallic cobalt can be kept away from the interface between substrate and diamond. Besides, it can be seen that the main component elements of TEOS decomposition products are Si and O, which accords with the elements of a-SiO_2.

Figure 3 shows the XRD patterns of cemented carbide substrates with or without a-SiO_2 interlayers in the 2θ range from 30° to 90°. As exhibited in Figs. 4(b)−(d), besides the diffraction peaks attributable to WC, weak diffraction peaks of silicon−cobalt compounds can also be detected with reflections at about 39.2° (Co_2Si), 43.3° (Co_2Si), 45.8° (CoSi), 47.7° ($CoSi_2$) and 50.2° (CoSi). This indicates that the surface residual Co on chemical etched cemented carbide substrates reacts with the a-SiO_2 material in CVD process, which is in accord with former study [12]. Moreover, for Specimens B, C and D, except for the diffraction peaks of WC and silicon−cobalt compounds, there are no other peaks in the XRD patterns, which means that the intermediate films are amorphous.

In order to further investigate the microstructure and phase composition of a-SiO_2 interlayer material, TEM analysis is applied. After sufficiently mechanical crushing, the interlayer material is ground into sub-microscale regimes. As shown in Figs. 4(a)−(d), dark spheroid particles of a-SiO_2 can be observed, with size between 100 and 200 nm. Moreover, it can be seen that bright spots exist in the particles. This indicates that the mirco-spheroid a-SiO_2 particles are hollow. And the size

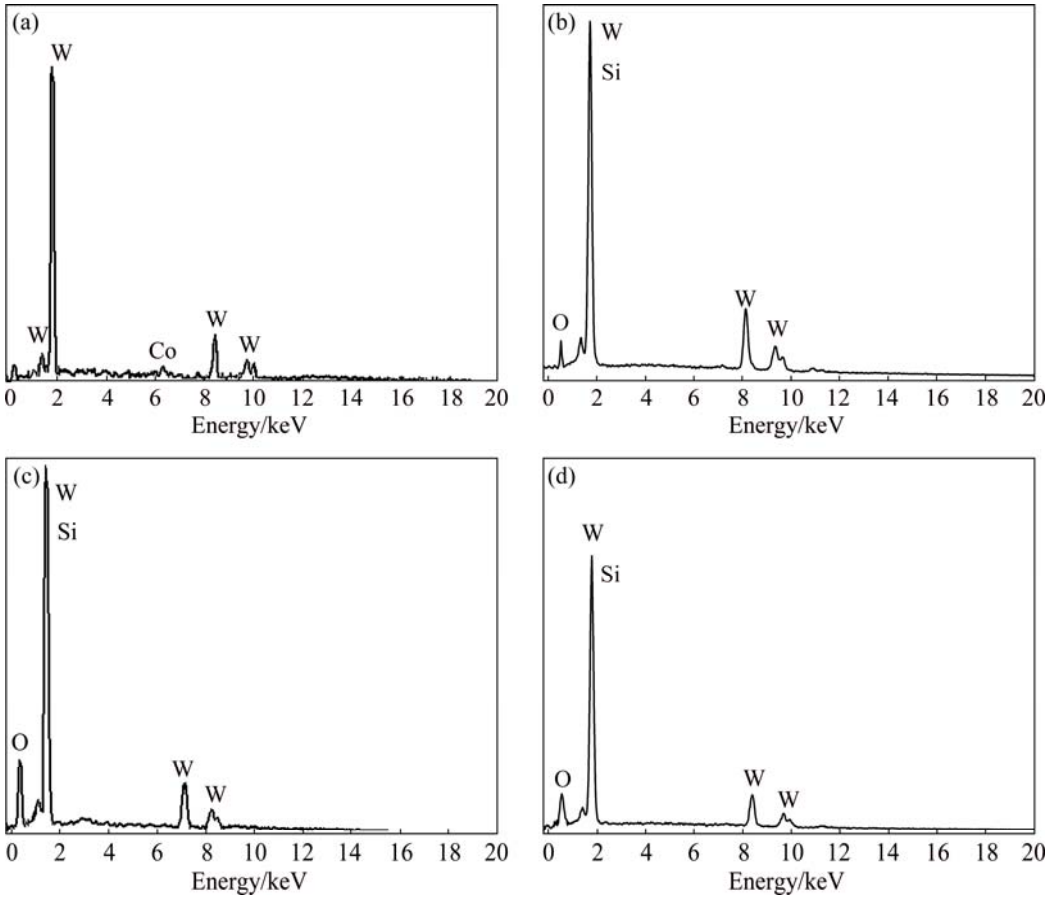

Fig. 2 EDX patterns of Specimen A (a), Specimen B (b), Specimen C (c) and Specimen D (d)

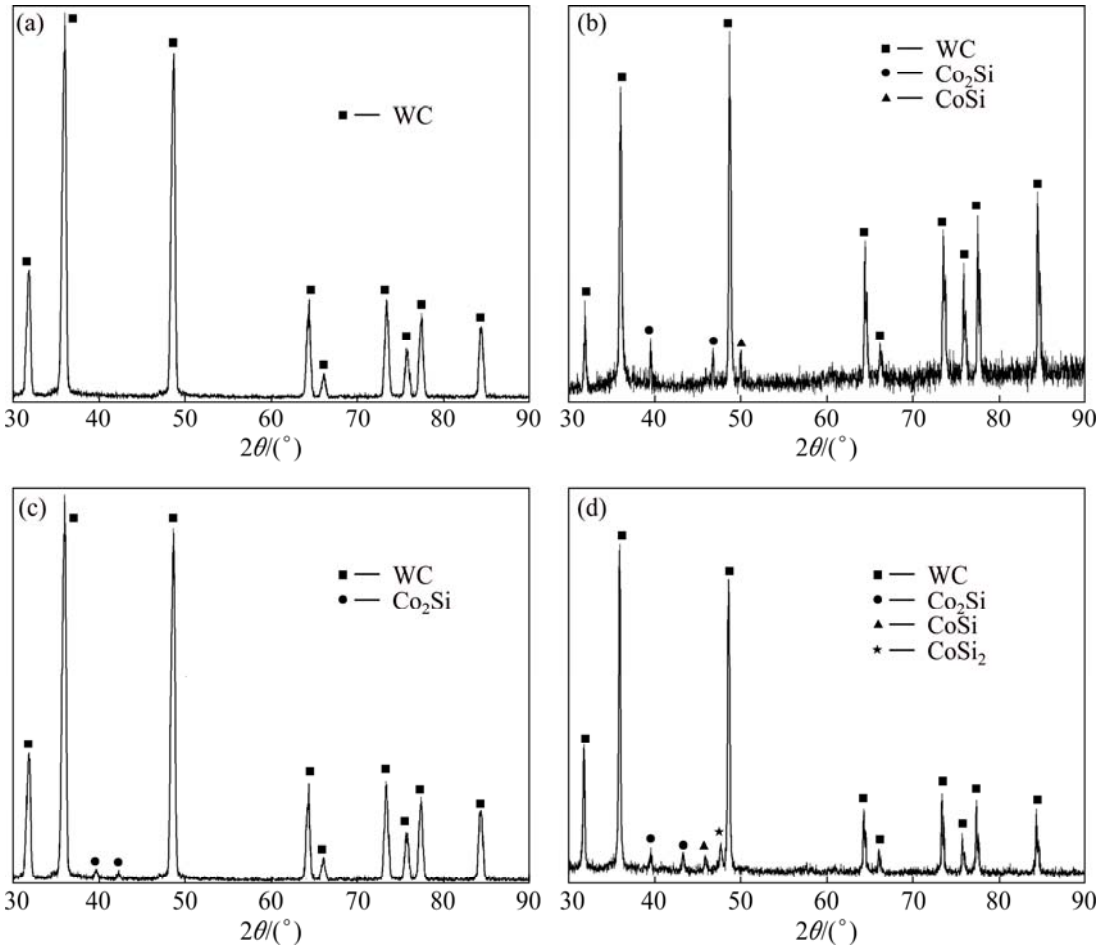

Fig. 3 XRD patterns of as-pretreated WC−Co substrates: (a) Specimen A; (b) Specimen B; (c) Specimen C; (d) Specimen D

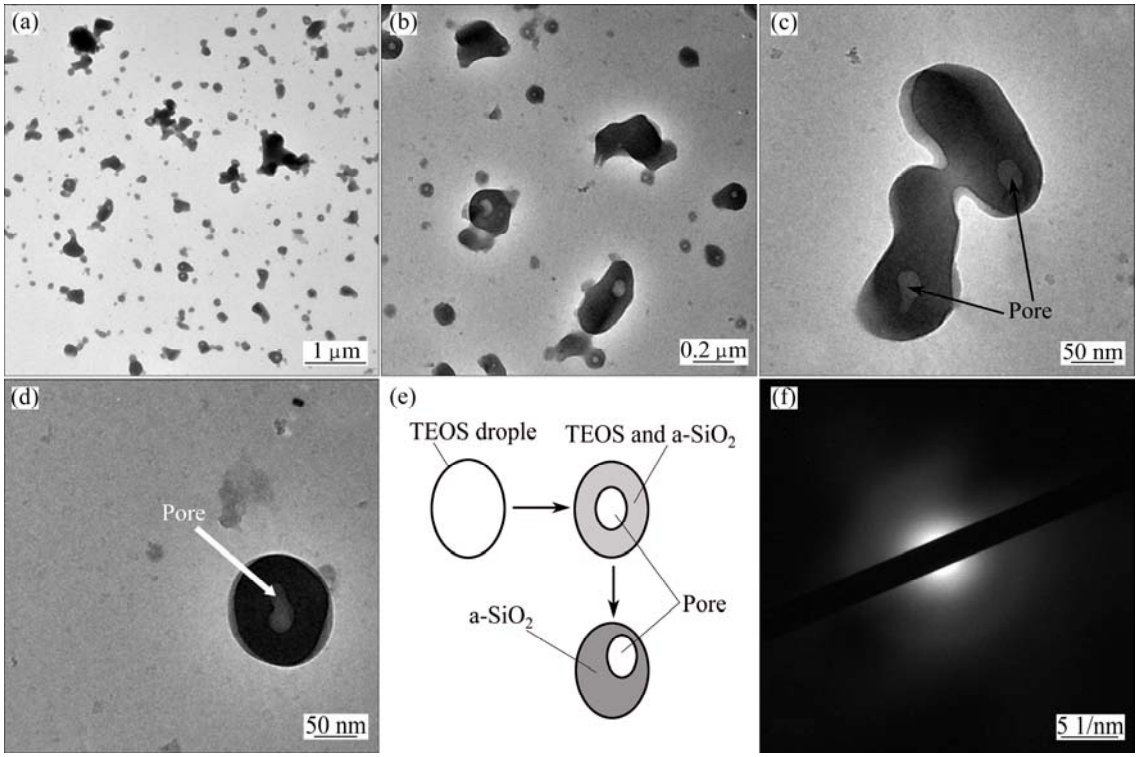

Fig. 4 TEM images of sub-microstructure of a-SiO_2 material (a−d), schematic illustration of formation of hollow micro-spheroid a-SiO_2 (e) and SAED pattern of interlayer material (f)

of hollow area is 30−50 nm. During the process of precursor pyrolysis, the TEOS vapor is led into the reaction chamber by H_2. It is a well-established fact that at elevated temperature (700 °C) and low pressure (1599.864 Pa), TEOS can convert to SiO_2: $Si(OC_2H_5)_4 \rightarrow SiO_2 + 2(C_2H_5)_2O$, the volatile coproduct being diethylether. As a result, the TEOS droplets disappear and a-SiO_2 particles come into being, which remain the shape of TEOS droplets. A small amount of diethylether may remain in each a-SiO_2 particle, which results in the hollow microstructure for each spheroid a-SiO_2 particle. Besides, it can be seen that the shape of hollow area is irregular and the hollow area seldom locates in the central region of each a-SiO_2 particle. This can be attributed to the flow of gaseous coproduct in the droplets. The schematic illustration of formation of hollow micro-spheroid a-SiO_2 is shown in Fig. 4(e). The selected area electron diffraction (SAED) pattern (Fig. 4(f)) of sub-microscale regimes consists of only broad and dull halos, confirming the presence of an amorphous structure. The TEM study illustrates that the a-SiO_2 film is formed by the accumulation of hollow micro-spheroid a-SiO_2 particles.

3.2 Quality identification of as-synthesized CVD diamond films

After deposition of 4 h, the pre-treated inserts are coated with continuous polycrystalline CVD diamond films. The SEM images of surface topography of as-synthesized CVD diamond films with or without amorphous cellular SiO_2 interlayers are shown in Fig. 5. For all four specimens, their morphologies are similar to each other. Pyramidal shaped (1 1 1) faceted crystallites can be observed in the films, whose size reaches 3−4 μm. Figure 6 shows the fractographs of Specimens E, F, G and H by SEM. Obviously, 3−4 μm-thick diamond film has been synthesized on each specimen. It can be observed in Fig. 6(b) that for the growth duration of 20 min, the mud-like a-SiO_2 interlayer is discontinuous. Moreover, for Specimen G, the a-SiO_2 film presents a ball-like appearance, with the thickness of about 0.4 μm. And for Specimen H, the a-SiO_2 interlayer shows a homogeneous amorphous microstructure, with the thickness of about 1 μm. This result is in good accordance with the surface topography study of a-SiO_2 films. WC grains can be obviously observed on the intermediate films in Figs. 6(b)−(d).

Figure 7 gives the XRD patterns of a-SiO_2 interlayer assisted diamond films with different interlayer growth durations. For all four specimens, (1 1 1) diamond peaks (at ~43.9°), (2 2 0) diamond peaks (at ~75.3°) and WC peaks can be clearly detected. Moreover, in Figs. 7(b)−(d), weak peaks at ~45.5°, 50.2° and 62.7° can be detected. The peak at ~50.2° is caused by $CoSi_2$. And the peaks at ~45.5° and 62.7° are ascribed to CoSi. These components are in good agreement with the XRD result of a-SiO_2 interlayers, as shown in Fig. 4. The disappearance of Co_2Si can be ascribed to the reaction of Co_2Si with Si in the amorphous material. According to Ref. [12], these silicon−cobalt compounds are expected to have no deleterious effects like metallic Co. No η phase (Co_3W_3C or Co_6W_6C) can be detected in Figs. 7(b)−(d). The thermal decomposition of TEOS droplets takes place near the hot filaments in the

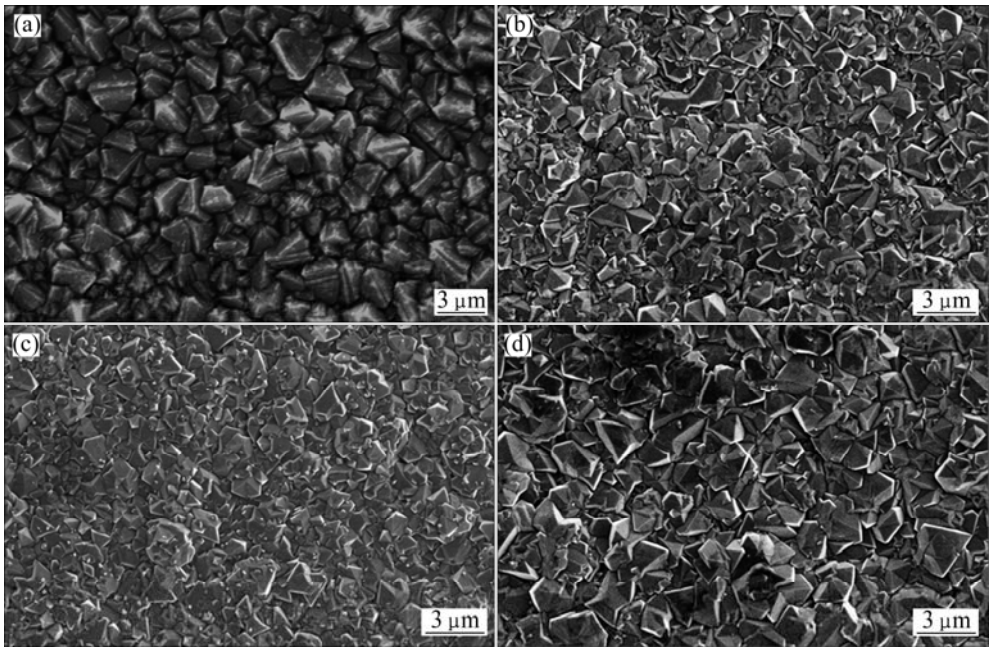

Fig. 5 SEM images of surface topography of as-fabricated CVD diamond films on Specimen E (a), Specimen F (b), Specimen G (c) and Specimen H (d)

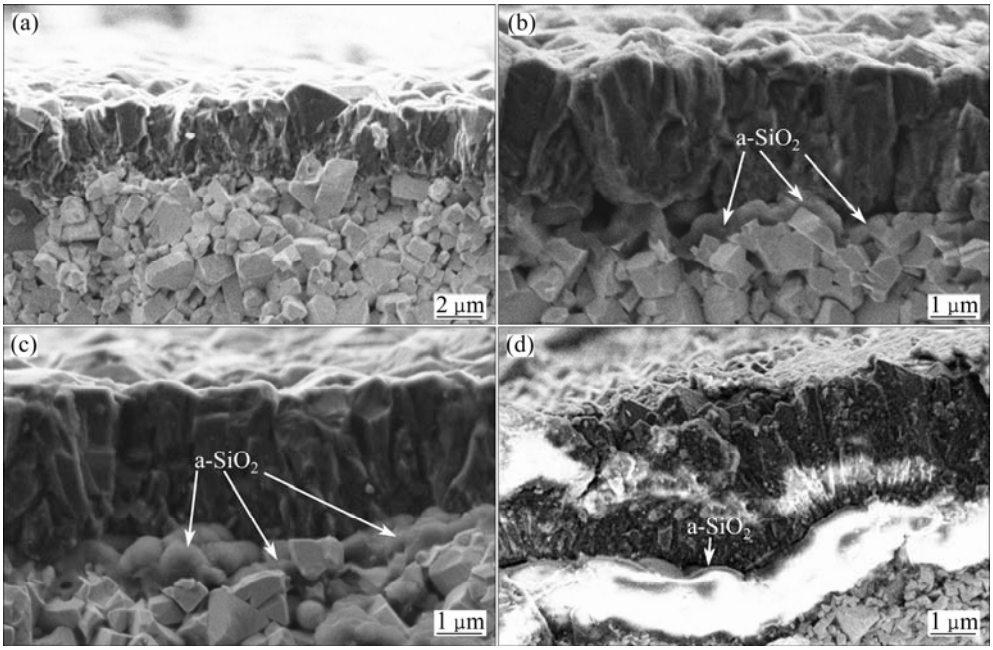

Fig. 6 SEM images showing fractographs of Specimen E (a), Specimen F (b), Specimen G (c) and Specimen H (d)

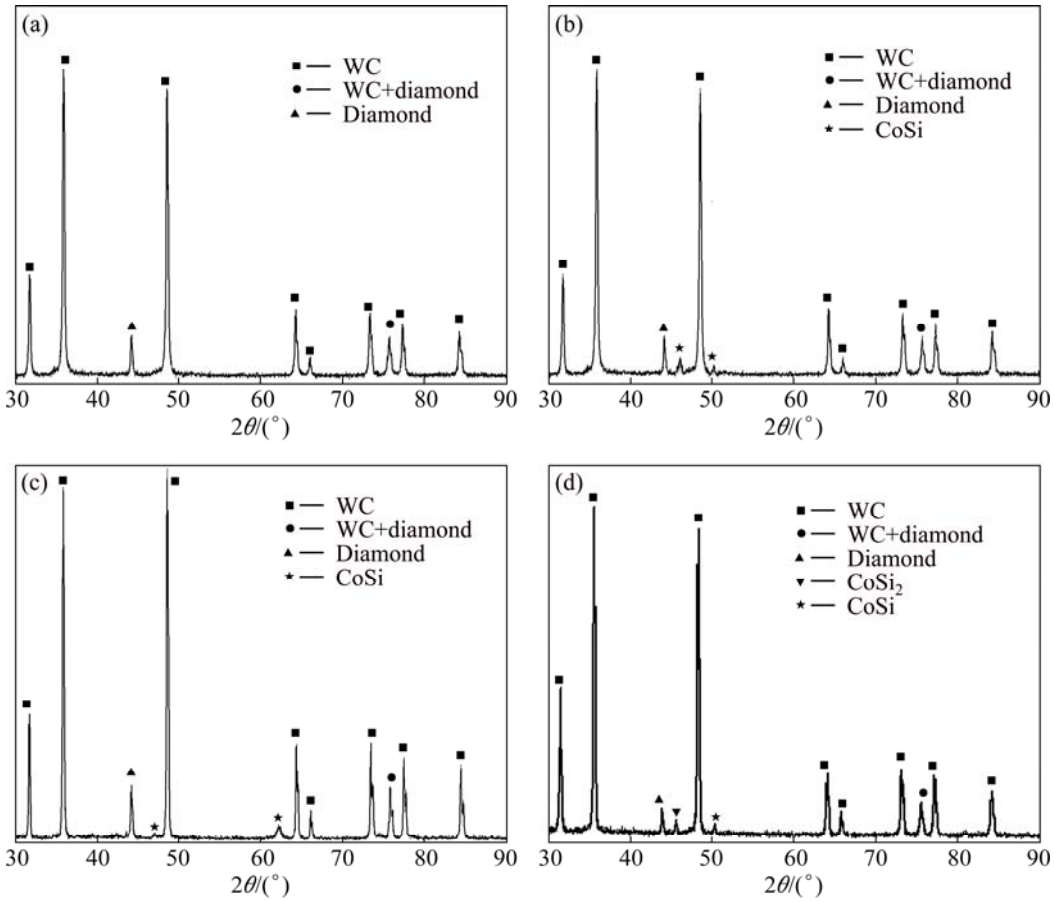

Fig. 7 XRD patterns of diamond films on Specimen E (a), Specimen F (b), Specimen G (c) and Specimen H (d)

atmosphere of H_2. Then, a-SiO_2 particles come into being, fall on WC−Co substrate and pile up. The CVD process of a-SiO_2 interlayer is performed above WC−Co substrate rather than on WC−Co substrate surface. So, the formation of η phase is avoided.

Figure 8 shows the micro-Raman spectra of as-fabricated diamond films. The intense band located at about 1332 cm^{-1} for each specimen is ascribed to

polycrystalline diamond. For Specimens E−G, the band between 1150 cm^{-1} and 1200 cm^{-1} can be ascribed to the presence of transpolyacetylene, and the broad band of relatively low intensity at about 1350 cm^{-1} is ascribed to D band (disordered carbon). Moreover, the band located at about 1600 cm^{-1} in the spectrum of Specimen H is referred to G band (graphite phase), and the broad band at 1450 cm^{-1} in the spectrum of Specimen E is attributed to transpolyacetylene as well [18−20].

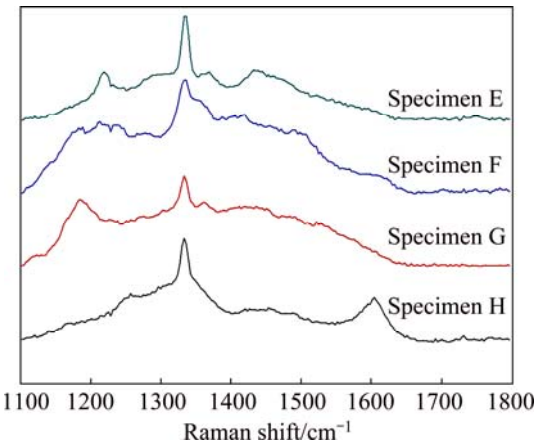

Fig. 8 Raman spectra of diamond films: (a) Specimen E; (b) Specimen F; (c) Specimen G; (d) Specimen H

3.3 Adhesion evaluation of as-fabricated diamond films

Indentation tests were conducted on Specimens E, F, G and H with a constant load of 100 kg, respectively. The SEM images of Rockwell indentations on Specimens E, F, G and H are presented in Fig. 9. As can be observed, the diamond film of Specimen E is severely flaked and chipped by indentation. In contrast, it can be seen that the indentation regions are circle in shape and there are no cracks extending from the indentations for the diamond films of Specimens F and G. No peelings occur in the a-SiO_2 interlayered diamond films. This result suggests that the adhesive strength of diamond films deposited on cemented carbide substrates can be remarkably enhanced when applying a-SiO_2 interlayers with growth durations of 20 min and 40 min. Especially for the diamond film of Specimen G, the diameter of the indentation crater is the smallest among all specimens, probably indicating the optimal adhesion of bi-layer (a-SiO_2 + diamond) films on WC−Co substrates. Nevertheless, Specimen H shows rather large scale flaking-off around the indentation region. Figure 9(d) shows that the adhesion of diamond film of Specimen H is not better than that of Specimen E. This probably means a rather poor adhesion between the a-SiO_2 interlayer (growth time of 60 min) and WC−Co substrate in comparison with that of Specimens E and F.

3.4 GFRP turning tests

In order to further investigate the influence of amorphous cellular SiO_2 interlayers on the cutting behavior of diamond films, cutting tests were conducted on as-fabricated diamond coated inserts assisted with a-SiO_2 interlayers. For comparison, CVD diamond coated insert with no interlayer (Specimen E) is also tested. The lifetime of the inserts is evaluated by their

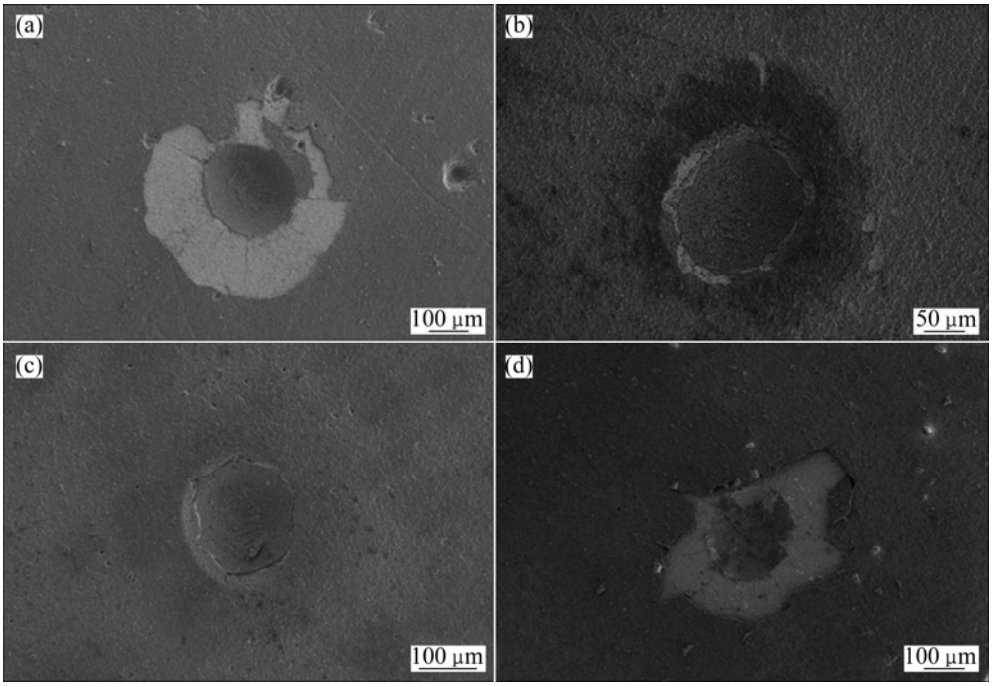

Fig. 9 SEM micrographs of delaminated area on as-fabricated diamond films: (a) Specimen E; (b) Specimen F; (c) Specimen G; (d) Specimen H

flank wear, and one insert will be considered as failure once its flank wear runs over 0.3 mm (according to Ref. [15]). Figure 10 shows the flank wear time evolution of CVD diamond coated inserts (Specimens E, F, G and H) in dry turning of GFRP. Figure 11 shows the flank wear of inserts observed by optical microscope. As exhibited in Fig. 10, the flank wear of Specimen E, i.e., conventional diamond coated insert without interlayer, firstly shows a slow increase from 0.04 to 0.14 mm for the first 6 min in machining GFRP. Afterwards, it rises sharply and surpasses 0.3 mm after machining for 9 min. Meanwhile, obvious flaking-off of the diamond film can be observed on Specimen E (Fig. 11). This suggests that the adhesive strength between the deposited diamond film and substrate plays a determinate role on the lifetime of diamond coated tool [15]. As for the a-SiO_2 interlayered diamond films with interlayer growth durations of 20 and 40 min, the flank wear rises very slowly. During the whole cutting test, the flank wear of both inserts is less than 0.2 mm. The diamond coated insert with a-SiO_2 interlayer for 40 min shows the least flank wear, whose flank wear is 0.15 mm. Moreover, there is no any sharp rise in flank wear, which is confirmed by the corresponding optical and SEM microscopes. As shown in Fig. 11, there is little

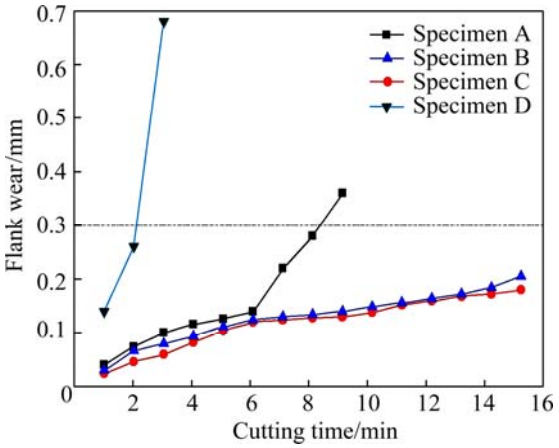

Fig. 10 Measured flank wear values for as-fabricated CVD diamond coated inserts

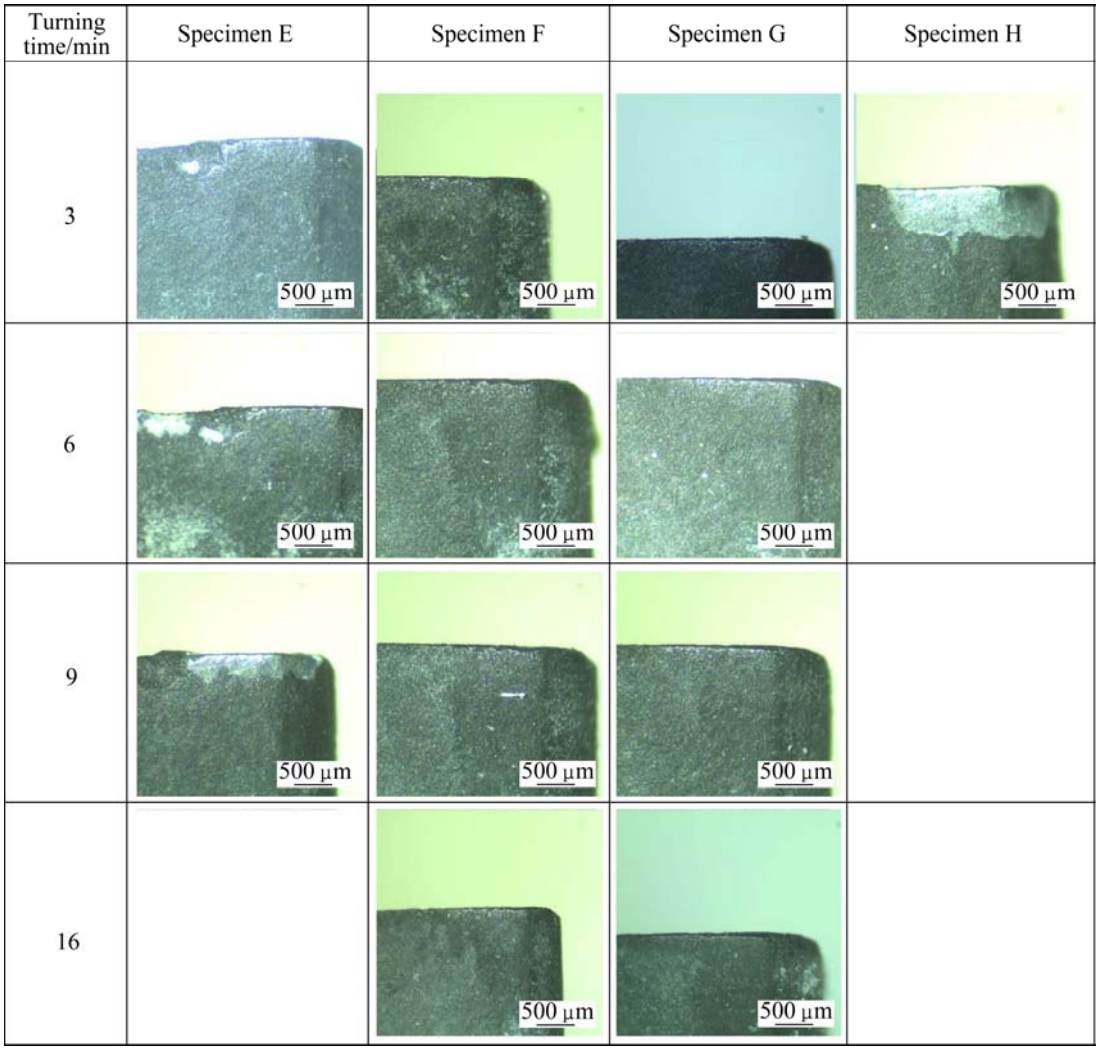

Fig. 11 Images of flank wear after turning

delamination on flank faces, which indicates the excellent performance of diamond coated cemented carbide inserts assisted with a-SiO_2 interlayers. The cutting performance of Specimen H is not better than that of Specimen E, which illustrates that the growth duration has a great influence on the effectiveness of a-SiO_2 interlayer. Figure 12 gives a further surface analysis of the worn area of Specimen H by SEM. It can be observed that the failure occurs at the interface between a-SiO_2 interlayer and WC−Co substrate, which shows the poor adhesion of a-SiO_2 interlayer with the growth duration of 1 h. This result is in good accordance with the former discussion.

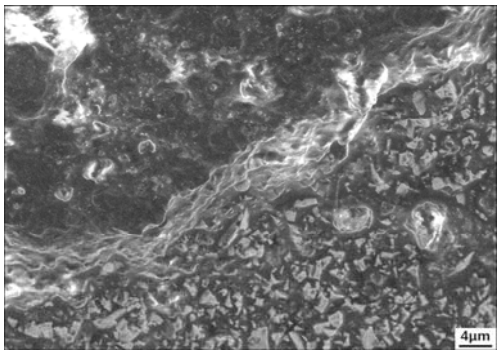

Fig. 12 SEM image of worn area of Specimen H after turning GFRP for 3 min

4 Discussion

There are mainly two factors for the adhesion enhancement of CVD diamond films on cemented carbide inserts by employing a-SiO_2 interlayers. They are discussed as follows.

On one hand, the a-SiO_2 interlayers can block the diffusion of Co and avoid its graphitization effect. The above EDX study shows that the conventional chemical etching cannot completely remove the surface binder phase of cemented carbide inserts. Also, during CVD diamond film growth, the diffusion of metallic cobalt towards film−substrate interface is unavoidable. The binder phase will attack the growing diamond crystallites, which leads to graphitization at the interface of film−substrate system and reduces the adhesion of CVD diamond films [3]. In contrast, when the a-SiO_2 interlayer is employed, the binder phase will react with a-SiO_2 material and be isolated from diamond film, as illustrated in Fig. 7. And thus the graphitization caused by Co can be remarkably reduced by the a-SiO_2 interlayer.

On the other hand, the a-SiO_2 interlayers can ensure a good bonding in the bi-layer (a-SiO_2 + diamond) film−substrate system. During the deposition of diamond films, the a-SiO_2 interlayers can react with H_2 and convert to H_2O and silicon. The silicon on the surface of a-SiO_2 interlayers can react with the hydrocarbon in the atmosphere. Si−C bonds will consequently come into being at the interface between diamond films and a-SiO_2 interlayers, which can ensure a good bonding of diamond crystallites on a-SiO_2 interlayer. Besides, after chemical etching, a porous, brittle and Co-depleted carbide layer can come into being on the WC−Co substrate surface, which is detrimental to the adhesion of diamond film. However, the a-SiO_2 material may act as amorphous binder to fill up the space among the brittle WC particles, improve the mechanical properties of substrate surface and the adhesion of diamond films.

However, it is worth noting that long growth duration (60 min) of a-SiO_2 interlayer can lead to a decreasing adhesion between a-SiO_2 interlayer and WC−Co substrate, as shown in the adhesion evaluation and GFRP turning test of Specimen H. The silicon−cobalt compounds, which are the reaction products of a-SiO_2 and residual binder phase, are very brittle. Moreover, the fracture toughness of as-synthesized a-SiO_2 material is limited. With the increase of growth duration, the interlayer thickness and the amount of silicon−cobalt compounds will increase as well. As a result, adhesion deterioration of the intermediate film will occur once beyond a crucial deposition duration with respect to the film thickness and the amount of silicon−cobalt compounds, which results in the insufficient adhesion of bi-layer (a-SiO_2 + diamond) film. Therefore, the deposition durations of a-SiO_2 interlayers are of great importance to the interfacial adhesion of film−substrate system in this work.

5 Conclusions

1) The SAED pattern of a-SiO_2 interlayer material illustrates only broad and dull halos, confirming that the intermediate film is amorphous. XRD study shows that silicon−cobalt compounds form at the interface between a-SiO_2 films and WC−Co substrates. Moreover, it can be observed by TEM that the a-SiO_2 films are composed of hollow micro-spheroid a-SiO_2 particles.

2) The indentation and cutting tests show that the adhesion and wear resistance of bi-layer (a-SiO_2 + diamond) films on WC−Co inserts are greatly improved in comparison with the diamond films directly deposited on WC−Co inserts. The a-SiO_2 interlayers can block the diffusion of Co and ensure a good bonding in the film−substrate system.

3) Adhesion deterioration of a-SiO_2 film will occur once beyond a crucial deposition duration with respect to the increasing interlayer thickness and increasing amount of silicon−cobalt compounds, which results in the

insufficient adhesion of bi-layer (a-SiO_2 + diamond) film. Thus, the growth duration of a-SiO_2 interlayer has a great influence on the adhesion of bi-layer (a-SiO_2 + diamond) film on the cemented carbide substrate. The a-SiO_2 interlayer film with growth duration of 40 min is found to ensure the best interfacial adhesion of film−substrate system.

References

[1] INSPEKTOR A, OLES E J, BAUER C E. Theory and practice in diamond coated metal-cutting tools [J]. International Journal of Refractory Metals and Hard Materials, 1997, 15: 49−56.

[2] SAIJO K, YAGI M, SHIBUKI K, TAKATSU S. The improvement of the adhesion strength of diamond films [J]. Surface and Coatings Technology, 1990, 43−44: 30−40.

[3] MALLIKA K, KOMANDURI R. Diamond coatings on cemented tungsten carbide tools by low-pressure microwave CVD [J]. Wear, 1999, 224: 245−266.

[4] TANG W, WANG S, LU F. Preparation and performance of diamond coatings on cemented carbide inserts with cobalt boride interlayers [J]. Diamond and Related Materials, 2000, 9: 1744−1748.

[5] TANG W, WANG Q, WANG S, LU F. Adherent diamond coatings on cemented carbide substrates with different cobalt contents [J]. Diamond and Related Materials, 2001, 10: 1700−1704.

[6] TANG W, WANG Q, WANG S, LU F. A comparison in performance of diamond coated cemented carbide cutting tools with and without a boride interlayer [J]. Surface and Coatings Technology, 2002, 153: 298−303.

[7] PETERS M, CUMMINGS R. Methods for coating adherent diamond films on cemented tungsten carbide substrates: Europe, 0519587 A1 [P]. 1992−12−23.

[8] ENDLER I, LEONHARDT A, SCHEIBE H, BORN R. Interlayers for diamond deposition on tool materials [J]. Diamond and Related Materials, 1996, 5: 299−303.

[9] DEUERLER F, BERG H, TABERSKY R, FREUNDLIEB A, PIES M, BUCK V. Pretreatment of substrate surface for improved adhesion of diamond films on hard metal cutting tools [J]. Diamond and Related Materials, 1996, 5: 1478−1489.

[10] POLINI R, MANTINI F, BARLETTA M, VALLE R, CASADEI F. Hot filament chemical vapour deposition and wear resistance of diamond films on WC−Co substrates coated using PVD-arc deposition technique [J]. Diamond and Related Materials, 2006, 15: 1284−1291.

[11] LI Y, TANG Y, YANG Q, SHIMADA S, WEI R, LEE K, HIROSE A. Al-enhanced nucleation and adhesion of diamond films on WC–Co substrates [J]. International Journal of Refractory Metals and Hard Materials, 2008, 26: 465−471.

[12] CABRAL G, GABLER J, LINDNER J, GRACIO J, POLINI R. A study of diamond film deposition on WC-Co inserts for graphite machining: Effectiveness of SiC interlayers prepared by HFCVD [J]. Diamond and Related Materials, 2008, 17: 1008−1014.

[13] BALDUS H, JANSEN M. Novel high-performance ceramics—Amorphous inorganic networks from molecular precursors [J]. Angewandte Chemie, 1997, 36: 328−343.

[14] PICKRELL D, ZHU W, BADZIAN A, NEWNHAM R, MASSIER R. Near-interface characterization of diamond films on silica and silicon [J]. Journal of Materials Research, 1991, 6: 1264−1277.

[15] ZHANG D, SHEN B, SUN F. Study on tribological behavior and cutting performance of CVD diamond and DLC films on Co-cemented tungsten carbide substrates [J]. Applied Surface Science, 2010, 256: 2479−2489.

[16] SUN F, ZHANG Z, CHEN M, SHEN H. Improvement of adhesive strength and surface roughness of diamond films on Co-cemented tungsten carbide tools [J]. Diamond and Related Materials, 2003, 12: 711−718.

[17] CAPPELLI E, PINZARI F, ASCARELLI P, RIGHINI G. Diamond nucleation and growth on different cutting tool materials: Influence of substrate pre-treatments [J]. Diamond and Related Materials, 1996, 5: 292−298.

[18] YOSHIKAWA M, MORI Y, OBATA H, MAEGAWA M, KATAGIRI G, ISHIDA H, ISHITANI A. Raman scattering from nanometer-sized diamond [J]. Applied Physics Letters, 1995, 67: 694−696.

[19] FERRARI A, ROBERTSON J. Rosonant Raman spectroscopy of disordered, amorphous, and diamond like carbon [J]. Physics Review B, 2001, 64: 075414.

[20] FERRARI A, ROBERTSON J. Origin of the 1150 cm^{-1} Raman mode in nanocrystalline diamond [J]. Physics Review B, 2001, 63: 121405.

基于非晶 SiO_2 过渡层在硬质合金刀具基体上沉积金刚石涂层

崔雨潇，赵天奇，孙方宏，沈 彬

上海交通大学 机械与动力工程学院 机械系统与振动国家重点实验室，上海 200240

摘 要：以氢气和正硅酸乙酯为反应源，采用前驱体裂解的方法在硬质合金基体上制备非晶 SiO_2(a-SiO_2)薄膜。X射线衍射(XRD)分析表明，非晶薄膜与基体发生反应，并在界面上形成硅钴化合物。此外，透射电镜(TEM)表征表明，该薄膜由微米级的空心球团状的非晶 SiO_2 颗粒构成。随后，将非晶 SiO_2 薄膜作为过渡层，采用热丝化学气相沉积技术在过渡层上沉积金刚石涂层。通过压痕试验表征制备获得的金刚石−非晶 SiO_2 复合涂层对硬质合金基体的附着力。通过加工玻璃丝纤维增强塑料(GFRP)表征该复合涂层的切削性能。结果表明，非晶 SiO_2 过渡层可以有效地改善金刚石涂层对硬质合金基体的附着力。此外，非晶 SiO_2 过渡层的厚度对金刚石涂层附着力的提升效果有很大影响。

关键词：热丝化学气相沉积法；金刚石薄膜；硬质合金；过渡层；附着力

(Edited by Xiang-qun LI)